

# Simultaneous X-ray and infrared variability in the quasar 3C273

Ian McHardy<sup>1</sup>, Anthony Lawson<sup>1</sup>, Andrew Newsam<sup>1,2</sup>, Alan Marscher<sup>3</sup>,  
Ian Robson<sup>4</sup>, Jason Stevens<sup>5</sup>

<sup>1</sup> *Department of Physics and Astronomy, University of Southampton, SO17 1BJ.*

<sup>2</sup> *Liverpool John Moores University, Astrophysics Research Institute, Birkenhead CH41 1LD*

<sup>3</sup> *Department of Astronomy, Boston University, Boston, MA, 02215, USA.*

<sup>4</sup> *Joint Astronomy Center, Hilo, HI 96720, USA.*

<sup>5</sup> *Mullard Space Science Laboratory, UCL, Holmbury St Mary, Surrey, RH5 6NT.*

Accepted for publication in the MNRAS.

## ABSTRACT

From a combination of high quality X-ray observations from the NASA Rossi X-ray Timing Explorer (RXTE), and infrared observations from the UK Infrared Telescope (UKIRT) we show that the medium energy X-ray (3–20 keV) and near infrared fluxes in the quasar 3C273 are highly correlated. It is widely believed that the X-ray emission in quasars like 3C273 arises from Compton scattering of low energy seed photons and our observations provide the first reliable detection of correlated variations in 3C273 between the X-ray band and any lower energy band. For a realistic electron distribution we demonstrate that it is probable that each decade of the seed photon distribution from the mm to IR waveband contributes roughly equally to the medium energy X-ray flux. However the expected mm variations are too small to be detected above the noise, probably explaining the lack of success of previous searches for a correlation between X-ray and mm variations. In addition we show that the infrared leads the X-rays by  $0.75 \pm 0.25$  days. These observations rule out the ‘External Compton’ emission process for the production of the X-rays.

**Key words:** quasars: individual: 3C273 - galaxies: active - X-rays: galaxies

## 1 INTRODUCTION

It is generally supposed that the high energy emission from blazars – ie BL Lac objects and quasars which display some evidence of relativistic jets – arises from Compton scattering of low energy seed photons. However the evidence for this supposition is quite weak. There has been remarkably little progress, despite a great deal of observational effort, in determining the details of the high energy emission models. Various possibilities exist, all of which require that the scattering particles are the relativistic electrons in the jet. The most popular hypothesis is the Synchrotron Self-Compton (SSC) model in which the seed photons are the synchrotron photons from the jet, up-scattered by their parent electrons. Alternatively the seed photons may arise externally to the jet (the External Compton, EC, process) or, in a combination of the two models, photons from the jet may be mirrored back to the jet (the Mirror Compton, MC, model) from a gas cloud before scattering up to high energies. The various models make slightly different predictions about the lags between the seed and Compton-scattered variations, and about the relative amplitudes of the two components and so, in

principle, the models can be distinguished (eg see Ghisellini and Maraschi 1996 and Marscher 1996 for summaries of the predictions of the various models). Much observational effort has therefore been devoted to attempting to find correlated variability in the high and low energy bands.

In the SSC model, it has generally been expected that, as the peak of the synchrotron photon number spectrum lies in the mm band for most radio-selected blazars, the mm would provide the bulk of the seed photons and so would be well correlated with the X-ray emission. However in the case of 3C273, one of the brightest blazars, extensive searches have been carried out for a connection between the X-ray and millimetre bands on both daily (McHardy 1993) and monthly (Courvoisier *et al.* 1990; McHardy 1996) timescales but no correlation has been found. The SSC model may, however, be saved if the flaring synchrotron component is self-absorbed at wavelengths longer than  $\sim 1$  mm. We therefore undertook a search for a correlation between the X-ray and infrared emission in 3C273; previous observations (eg Courvoisier *et al.* 1990; Robson *et al.* 1993) have confirmed that infrared flares in 3C273 are due to variations in a syn-

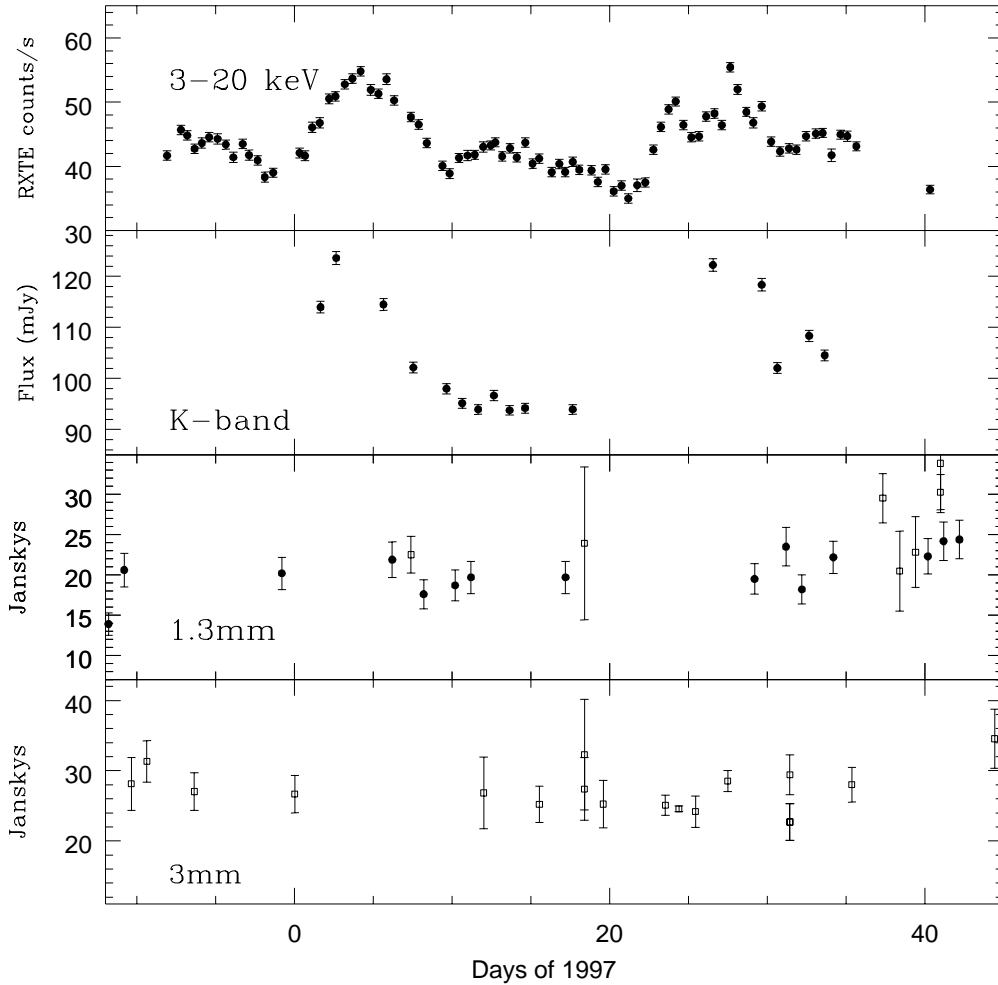


**Figure 1.** X-ray, infrared and millimetre lightcurves. The X-ray counts are the total from 3 PCUs of the PCA. The 1.3mm data are from the JCMT (filled circles), with some points from OVRO (open squares). The 3mm data are all from OVRO.

chrotron component. In the past, large amplitude infrared flares have been seen only rarely in 3C273 (eg Courvoisier *et al.* 1990; Robson *et al.* 1993), partially because of limited sampling which usually could not detect flares with overall timescales  $\sim$ week. Nonetheless the previous sampling was sufficient to show that such flare activity is not a continual occurrence. It may be relevant that the present observations, during which large amplitude infrared variability was detected, were made during a period when the millimetre flux from 3C273 was very high.

Here we present what we believe is the best sampled observation of correlated variability between the synchrotron and Compton-scattered wavebands in any blazar. The observations cover not just one flaring event, which could be due to chance, unrelated, flaring in the two wavebands, but two large variations. The observations, including the X-ray, infrared and millimetre lightcurves, and cross-correlation of the X-ray and other waveband lightcurves, are described in Section 2. The origin of the X-ray seed photons is discussed

in Section 3, the implications of the observations are discussed in Section 4 and the overall conclusions are given in Section 5.

## 2 OBSERVATIONS

### 2.1 X-ray Observations

During the 6 week period from 22 December 1996 to 5 February 1997, X-ray observations were carried out twice a day by RXTE and nightly near infrared service observations were made at the United Kingdom Infrared Telescope (UKIRT).

The X-ray observations were made with the large area ( $0.7 \text{ m}^2$ ) Proportional Counter Array (PCA) on RXTE (Bradt, Rothschild and Swank 1993). Each observation lasted for  $\sim 1$  ksec. The PCA is a non-imaging device with a field of view of FWHM  $\sim 1^\circ$  and so the background count rate was calculated using the RXTE q6 background model.

Standard selection criteria were applied to reject data of particularly high background contamination.

3C273 is detectable in each observation in the energy range 3-20 keV and its spectrum is well fitted by a simple power law. As with other PCA spectra (eg The Crab –see <http://lheawww.gsfc.nasa.gov/users/keith/pcarmf.html>) the measured energy index,  $\alpha=0.7$ , is 0.1 steeper than measured by previous experiments, eg GINGA (Turner *et al.* 1990). The X-ray spectra, and spectral variability during the present observations are discussed in detail by Lawson *et al.* (in preparation). The average count rate of 45 counts  $\text{s}^{-1}$  (3-20 keV) (the total for 3 of the proportional counter units, PCUs, of the PCA) corresponds to a flux of  $1.5 \times 10^{-10}$  ergs  $\text{cm}^{-2} \text{s}^{-1}$  (2-10 keV).

In figure 1 we present the count rate in the 3-20 keV band. We see two large X-ray flares. The first flare begins on approximately 1 January 1997, reaches a peak on 4 January and returns to its pre-flare level on 10 January. The flare is quite smooth. The second flare begins on 22 January and lasts until approximately 1 February. The initial rise is faster than that of the first flare, and the overall shape indicates a superposition of a number of smaller flares. X-ray spectral variations are seen during the flares (Lawson *et al.* in preparation), showing that changes in the Doppler factor of the jet cannot, alone, explain the observed variability.

## 2.2 Infrared and Millimetre Observations

In figure 1 we show 1.3 and 3 mm observations from the James Clerk Maxwell Telescope (JCMT - see Robson *et al.* 1993 for reduction details) and from the Owens Valley Radio Observatory (OVRO); the latter data were obtained from the calibration database. There is no evidence of flares of comparable amplitude to those in the X-ray lightcurve, but the sampling is poorer and the errors are larger.

We also show the K-band lightcurve derived from service observations at the United Kingdom Infrared Telescope (UKIRT) from 1 January until 3 February 1997. The observations were made with the infrared imaging camera IR-CAM3 with typical exposures of 3 minutes. The observations were made in a standard mosaic manner and the data were also reduced in a standard manner. There are some gaps due to poor weather but increases in the infrared flux at the same time as the X-ray flares can be seen clearly. The average K error is  $\sim 1\text{mJy}$  (ie 1 per cent). Approximately half of the error comes from the Poisson noise and the rest comes from calibration uncertainties.

## 2.3 X-ray/Infrared Cross-Correlation

We have cross-correlated the X-ray lightcurves with the millimetre and K-band lightcurves using the Edelson and Krolik (1988) discrete cross-correlation algorithm as coded by Bruce Peterson (private communication). As found previously there is no correlation of the X-ray emission with the millimetre emission but there is a very strong correlation with the infrared emission (figure 2) with correlation coefficient close to unity. The cross-correlation peaks close to zero days lag but is asymmetric. Although we can rule out the infrared lagging the X-rays by more than about one day, a lag of the infrared by the X-rays by up to 5 days is possible.

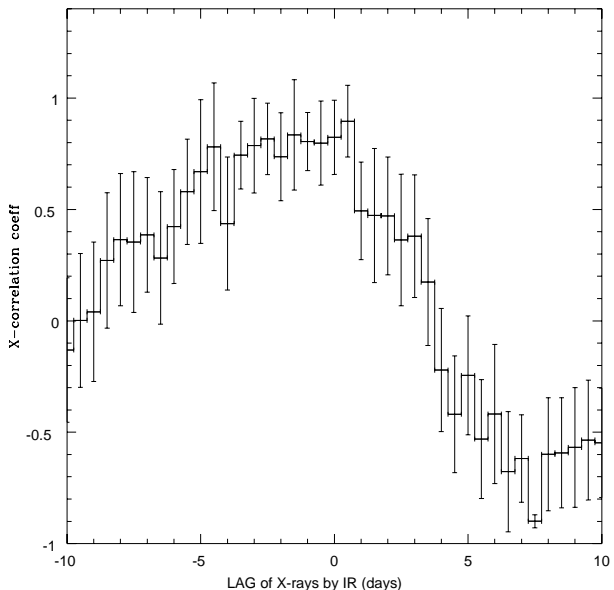


**Figure 2.** Cross-correlation of the 3-20 keV X-ray lightcurve and K-band lightcurves shown in figure 1.

The observations presented here are the first to show a definite correlation in 3C273 between the X-ray emission and that of any potential seed photons.

## 3 THE ORIGIN OF THE X-RAY SEED PHOTONS

An important question is whether the infrared photons are actually the seed photons for the X-ray emission or whether they are simply tracers of a more extended spectral continuum, with the X-rays arising from scattering of another part of the continuum. Robson *et al.* (1993) state that in 3C273 the onset and peak of flares occur more or less simultaneously (ie lags of  $< 1$  day) from K-band to 1.1 mm. Therefore although we have not adequately monitored at wavelengths longer than  $2.2\mu$ , we assume that the whole IR to mm continuum does rise simultaneously.

We have therefore calculated the Compton scattered spectrum resulting from the scattering of individual decades of seed photon energies, from the infrared to millimetre bands. The seed photons are taken from a typical photon distribution and are scattered by a typical electron distribution. The resulting scattered spectra are shown in figure 3 and details of the photon and electron distributions are given in the caption to figure 3. It is assumed that the emission region is optically thin which, in blazars, is true for the large majority of frequencies discussed in figure 3. Note that although the electron and input photon spectra are self-consistent as regards the SSC mechanism, the result is general and applies to scattering of seed photons produced by any mechanism. At the highest Compton scattered energies, ie GeV, only the highest energy seed photons below the break in the photon distribution (ie near infrared) are important. However at medium energy X-rays we get approximately equal con-

tributions from each decade of seed photons. Thus scattered infrared photons probably contribute about 20 per cent of the medium energy X-ray flux and the sum of the scattered X-ray emission from lower energy seed photons exceeds that from the infrared alone. These ratios can be altered slightly by different choices of seed photon and electron spectral index, but the general result is robust.

If the infrared is indeed a tracer of the seed photon continuum, we can extrapolate to find the expected variability in the millimetre band. The peak and minimum observed K fluxes during our observations are 124 and 93 mJy respectively, ie a range of 31 mJy, although we note that we do not have K observations at either the peak or minimum of the X-ray lightcurves and so the true range of K-band variability may be somewhat more. If the spectral index,  $\alpha$ , of the seed spectrum is 0.75 (as reported by Robson *et al.* and Stevens *et al.* 1998) we would then expect a rise of  $\sim 3.7$  Jy at 1.3 mm, which we cannot rule out in the present observations and which would not have been easy to detect in previous, less well sampled, monitoring observations, explaining the lack of success of previous searches for millimetre/X-ray correlations. At 3mm the predicted variability amplitude would be 7 Jy. Robson *et al.* states that the 3mm rises lag 1mm rises by about 6 days, and 3mm decays are substantially longer, which would all make them easier to detect, given our sampling pattern. However, with the exception of the very last datapoint at day 44, no deviations of more than 5 Jy from the mean level are detected. The implication is that  $\alpha \leq 0.75$  or that the flaring component is self absorbed by 3mm. If the flaring component has  $\alpha = 1.2$  as derived for the 1983 flare by Marscher and Gear (1985), that component would have to be self absorbed by 1.3mm.

## 4 DISCUSSION

There are two major observational constraints on the X-ray emission mechanism: the relative amplitudes of the synchrotron and Compton scattered components, and the time lag between them. Here we attempt to constrain these parameters by modelling the X-ray lightcurve.

### 4.1 Modelling the X-ray lightcurve

If the X-ray emission is physically related to the infrared emission, then we can parameterise the relationship by:

$$X_{\text{predicted}}(t) = A(K_{\text{flux}}(t - \delta t) - K_{\text{quiescent}})^N + X_{\text{quiescent}}$$

$K_{\text{quiescent}}$  is a non-varying K-band component. Robson *et al.* (1993) show that such a component, steady on a timescale of years, is contributed probably by warm dust in the broad line clouds, heated to the point of evaporation. Following Robson *et al.* we fix  $K_{\text{quiescent}} = 50\text{mJy}$ .  $K_{\text{flux}}(t - \delta t)$  is the total observed K-band flux at time  $t - \delta t$  and  $X_{\text{predicted}}(t)$  is then the predicted total X-ray flux at time  $t$ .  $X_{\text{quiescent}}$  is the part of the X-ray flux which does not come from the flaring region. The variable  $\delta t$  is included to allow for lags between the X-ray and infrared variations. Initially we set  $\delta t = 0$  but, in section 4.2, we consider the implications of allowing  $\delta t$  to vary.  $A$  is the constant of proportionality (containing information about the electron density, magnetic field and the various flux conversion constants) and

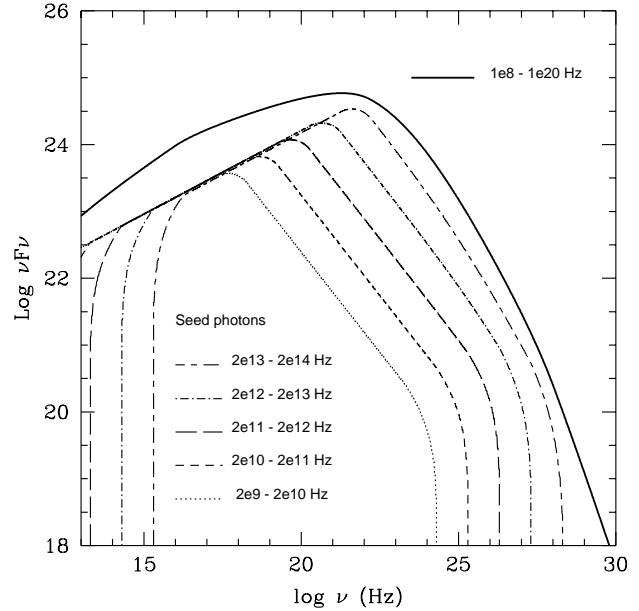


**Figure 3.** Compton scattered spectrum resulting from the scattering of a seed photon spectrum stretching from  $\nu = 10^8$  to  $10^{20}$  Hz. At low frequencies the spectral index,  $\alpha$ , where flux,  $F \propto \nu^{-\alpha}$ , is 0.75 and, above a break frequency of  $10^{14}$  Hz,  $\alpha = 1.5$ . The electron number energy spectrum,  $N(\gamma) \propto \gamma^{-m}$ , where  $\gamma$  is the Lorentz factor of the individual electrons, stretches from  $\gamma = 10$  to  $10^7$ , with a slope,  $m$ , at low energies of 2.5 and  $m = 4.0$  above  $\gamma = 10^4$ . The proper Klein-Nishina cross section is used. No bulk relativistic motion is included. The thick line represents the total scattered spectrum. The other lines represent the result of scattering seed photons with only one decade of energy. Note that, in the medium energy X-ray band ( $4 \text{ keV} = 10^{18} \text{ Hz}$ ), seed photons from all decades from cm to near infrared contribute equally to the scattered flux, with each contributing about 20 per cent.

$N$  contains information about the emission mechanism. For example if the X-rays arise from variations in electron density then we expect  $N = 2$  in the SSC and MC processes, but in the EC model  $N = 1$ . We have therefore performed a  $\chi^2$  fit, using a standard Levenburg-Marquardt minimisation routine, comparing the predicted X-ray flux with the observed flux, in order to determine the three unknowns,  $A$ ,  $X_{\text{quiescent}}$  and  $N$ . The errors on the predicted X-ray flux are derived from the observed errors on the infrared flux.

The present infrared lightcurve is not well enough sampled to determine all 3 parameters independently but, if  $X_{\text{quiescent}}$  could be determined precisely from other observations, then we could determine  $N$  to  $\pm 0.2$ . Here  $N$  varies from 0.5 for  $X_{\text{quiescent}} = 0$  to 1.0 for  $X_{\text{quiescent}} = 23$  and 2.0 for  $X_{\text{quiescent}} = 35$ . The minimum observed value of the total X-ray count rate during the present observations was  $35 \text{ count s}^{-1}$ . Hence as some part of those  $35 \text{ count s}^{-1}$  almost certainly comes from X-ray components which are not associated with the flaring activity, eg a Seyfert-like nucleus or other parts of the jet, then the maximum allowed value of  $N$  is probably just below 2. Typical RXTE count rates outside of major flaring periods are in the range 20–25 counts  $\text{s}^{-1}$  and fluxes observed by previous satellites (eg see Turner *et al.* 1990) correspond to the same flux range.

If that count rate represents the true value of  $X_{\text{quiescent}}$ , then  $N$  is probably nearer unity, favouring EC models, or SSC or MC models in which variations in the magnetic field strength play an important part in flux variations.

#### 4.2 Implications of lightcurve modelling for lags

Comparison of the best-fit predicted and observed X-ray fluxes reveals that, in the first flare, the predicted fluxes exceed the observed fluxes on the rise and the reverse is true on the fall. A better fit, at least for the first flare, occurs if the predicted lightcurve is delayed by about a day (in other words, the observed IR leads the X-rays). We therefore introduced a variety of time shifts,  $\delta t$  above, into the IR lightcurve, and also separately considered the first and second flares, and refitted. We applied simple linear interpolation to estimate the IR flux at the exact (shifted) time of the X-ray observations. The results are shown in figure 4.

When considering all of the IR data, we obtain a plot (top panel of figure 4) which is rather similar to the cross-correlation plot (figure 2), which is not too surprising as the analysis techniques are similar, although the modelling in principle allows us to quantify the goodness of fit. We are cautious of overinterpreting the above datasets and so, we prefer to plot figure 4 in terms of raw  $\chi^2$  rather than probabilities which might be taken too literally. As in many analyses where the errors are small, slight (real) differences in data streams lead to low probabilities of agreement even though overall agreement is very good. Here a minor variation in either X-rays or IR from a region not associated with the flare could provide that small difference. However the change in relative goodness of fit can be easily seen from the  $\chi^2$  plots. When we consider separately the IR data from the first flare (ie the 11 data points up to day 20 of 1997), or from the second flare (the remaining 5 data points) we obtain much better fits. We find that the first flare is best fitted if the IR leads the X-rays by about 0.75 days. We are again cautious in ascribing exact errors to the lag but changes of  $\delta\chi^2$  of 6.4, corresponding to 40 per cent confidence, occur in the first flare at 0.25 days from the minimum value. A lag of the X-rays by the IR by less than 0.25 days is ruled out at the 99.97 per cent confidence level. The more limited data of the second flare is, however, best fitted by simultaneous IR and X-ray variations.

Again with caution, we note that Lawson *et al.* (in preparation) find different X-ray spectral behaviour between the two flares. In the first flare the spectrum hardens at the flare onset but, at the peak, the spectrum is softer than the time averaged spectrum; in the second flare the hardness tracks the flux quite closely with the hardest emission corresponding to the peak flux. Thus there do appear to be differences between the two flares. However whether the observed differences are due to differences in, for example the physical parameters of the emitting region (eg density, magnetic field strength), the strength of any exciting shock, or the geometry of the emitting regions, is not yet clear but is an interesting subject for future investigations.

Although not really intended for such analysis, blind application of Keith Horne's Maximum Entropy Echo Mapping software to the whole dataset also leads to the conclusion that the IR leads the X-rays by 0.75 days (Horne, private communication).

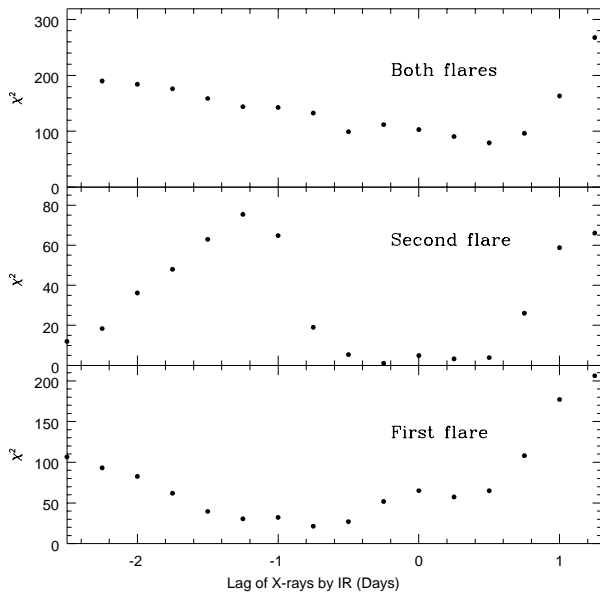


**Figure 4.** Results of comparing the observed X-ray lightcurve with that predicted from the infrared variations, with all parameters allowed to remain free apart from the X-ray/infrared lag. The numbers of degrees of freedom are 13 (both flares), 8 (first flare) and 2 (second flare). Note that it is impossible to obtain a good fit to both X-ray flares simultaneously but acceptable fits can be obtained to both fits individually. However the lags are different for the two flares with the X-rays lagging the infrared by  $\sim 0.75$  days in the first flare but the X-rays and infrared being approximately simultaneous in the second flare.

As an example we show, in figure 5, the observed X-ray lightcurve and the predicted lightcurve, based on parameters derived from fitting to just the first flare with the IR leading by 0.75 days (the best fit). We see that such a lag does not fit the second flare well. In particular the predicted X-ray fluxes for the second flare all lie above the observed fluxes by about 4 counts  $\text{s}^{-1}$  and the predicted fluxes now slightly lag (by about half a day) the observed fluxes. One possible explanation of the excess is that  $X_{\text{quiescent}}$  is lower during the second flare. From our long term weekly monitoring (in preparation) we note that the two flares shown here are actually superposed on a slowly decreasing trend of the correct slope to explain the excess. Inclusion of such a trend into our fitting procedure does produce a slightly better fit for the overall dataset, but the different lags between the first and second flare still prevent a good overall fit from being obtained. We therefore favour the explanation that the long term lightcurve is actually made up of a number of short timescale (week) flares, superposed on a more slowly varying (months) ‘quiescent’ component, rather than proposing that the lightcurve is made up entirely of short flares, with no underlying ‘quiescent’ component.

#### 4.3 The X-ray Emission Mechanism

The similarity between the present infrared variations and those of previous infrared variations where the whole IR to

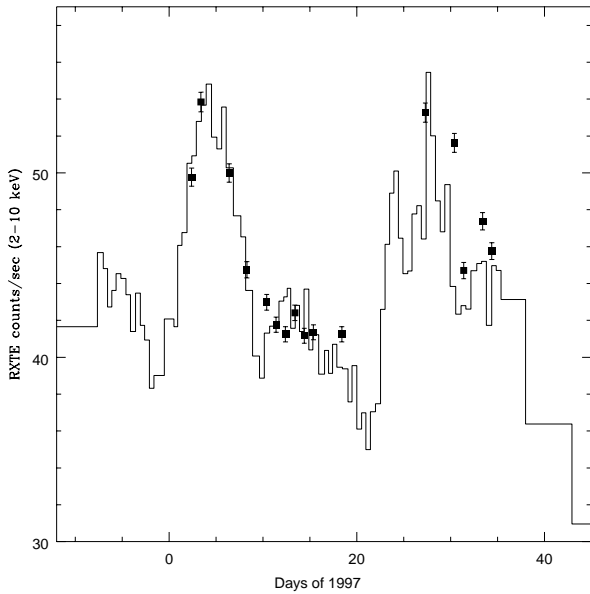


**Figure 5.** Observed X-ray lightcurve (histogram) and the best fit predicted X-ray flux (filled squares) based on the parameters derived from fitting the infrared observations to the first flare (11 data points) only. The best-fit parameters are  $A = 0.47$ ,  $N = 0.98$  and  $X_{quiescent} = 22.1$ . Following from figure 4 the lead of the IR over the observed X-rays is fixed at 0.75 days, the best-fit value for the first flare. The observed X-ray errorbars (see figure 1) are not repeated here to avoid cluttering the diagram. Note how the predicted X-ray fluxes for the second ‘flare’ are then systematically overestimated and also slightly lag the observed X-ray fluxes.

mm continuum varied together (Robson *et al.* 1993), and the lack of any other likely source of rapidly variable infrared radiation, means that the varying component of the infrared flux is almost certainly synchrotron radiation from the jet. The very strong correlation between the X-ray and infrared lightcurves shows that the same electrons which produce the infrared synchrotron emission must also produce the scattered X-ray emission. The original version of the EC model (Dermer and Schlickeiser 1993) in which the high energy variations are caused by variations in the external seed photons is thus ruled out. The next version, in which the electrons in the jet which produce the infrared synchrotron emission also scatter an all-pervading ambient nuclear photon field (Sikora, Begelman and Rees 1994) is also ruled out, at least for the first flare, as we would then expect exactly simultaneous X-ray and infrared variations.

The remaining possible emission mechanisms are the SSC process, which must occur at some level, and the MC process. In the SSC process we expect, for moderate variations such as those observed here where the emission region probably remains optically thin, that the X-ray flares will lag the IR flares (in the source frame) by approximately the light travel time across the radius of the emission region. The lag is because most photons will not be scattered where they are produced but will typically travel the radius of the emission region before being scattered. In this model we can

therefore deduce the radius if we know the bulk Lorentz factor of the jet. In the MC model the low energy photons also lead the high energy photons, in this case by approximately the light travel time between the emission region in the jet and the cloud. If the cloud forms part of the broad line region we might reasonably expect lags of order days.

The EC model is ruled out by the IR/X-ray lag but both the SSC and MC models are consistent with the lag. The parameter  $N$  is not yet well defined but the present indications are that it is closer to 1 than to 2, which, for the SSC and MC models, implies that changes in magnetic field strength are at least partially responsible for the observed variations. The MC compton scattered flux has a higher dependence on the bulk Lorentz factor of the jet than does the SSC mechanism, but that factor is very hard to measure.

## 5 CONCLUSIONS

We have demonstrated, for the first time, a strong relationship between the X-ray emission and that in any other lower frequency band in 3C273. We have shown that the IR and X-ray emission in 3C273 are very strongly correlated. By means of a simple calculation we have shown that each decade of the synchrotron spectrum from the cm to IR bands probably contributes equally (at about 20 per cent per decade) to the Compton scattered X-ray flux. Overall the lag between the IR and X-ray bands is very small but, in at least the first flare, the IR leads the X-ray emission by  $\sim 0.75 \pm 0.25$  days. This lag rules out the EC model but is consistent with either the SSC or MC model.

We have attempted to measure the parameter  $N$  which determines the relationship between the seed photon and Compton scattered flux. The present data do not greatly constrain  $N$  although they indicate that 2 is the absolute upper limit and that a lower value is probable. In terms of the SSC or MC models the implication is that changes in the magnetic field strength are responsible for at least part of the observed variations and, for  $N = 1$ , could be responsible for all of the variations.

Because of their intrinsic similarity, the SSC and MC models are hard to distinguish. However if it were possible to measure IR/X-ray lags for a number of flares, of similar amplitude, in the same source, then in the SSC model one would expect broadly similar lags in each case, assuming that the emission comes from physically similar emission regions. However in the MC model the reflecting clouds will probably be at a variety of different distances and so the lags should be different in each case.

We may also examine variations in optical and UV emission line strength. If synchrotron radiation from the jet is irradiating surrounding clouds (MC process), then we would expect the resultant recombination line radiation to vary with similar amplitude to, and simultaneously with, the synchrotron emission. However in the SSC process we would expect no change in emission line strength.

Further X-ray/IR observations with  $\sim$ few hour time resolution are required to refine the lag found here and to determine whether the lag is different in different flares.

**Acknowledgements** We are very pleased to thank the management and operational staff of both RXTE and

UKIRT for their cooperation in scheduling and carrying out these observations. We thank Keith Horne for running our data through his MEMECHO software. IM<sup>c</sup>H thanks PPARC for grant support and APM was supported in part by NASA Astrophysical Theory Grant NAG5-3839.

## REFERENCES

- Bradt, H.V.D, Rothschild, R.E. and Swank, J.H., 1993. A&AS, 97, 355.
- Courvoisier, T.J-L. *et al.* 1990. A&A 234 73.
- Dermer, C.D. and Schlickeiser, R., 1993. ApJ, 416, 458.
- Edelson, R.A. and Krolik, J., 1988. ApJ, 333, 646.
- Ghisellini, G. and Maraschi, L., 1996. ASP Conf. Series, 110, 436.
- Marscher, A.P. and Gear, W.K., 1985. ApJ, 298, 1114.
- Marscher, A.P., 1996. ASP Conf. Series, 110, 248.
- M<sup>c</sup>Hardy, I.M., 1993. Proc IAU Symposium 159, eds Courvoisier, T. and Blecha, A., Kluwer, p193.
- M<sup>c</sup>Hardy, I.M., 1996. ASP Conf. Series, 110, 293.
- Robson, E.I. *et al.* , 1993. MNRAS, 262, 249.
- Sikora, M. and Begelman, M.C. and Rees, M.J., 1994. ApJ, 421, 153.
- Stevens, J., Robson, I., Gear, W., Cawthorne, T., Aller, M., Aller, H., Terasranta, H. and Wright, M., 1998, ApJ 502, 182.
- Turner, M.J.L. *et al.* 1990. MNRAS,